

## Fluctuation power spectra reveal dynamical heterogeneity of peptides

Bhavin Khatri,<sup>1</sup> Zu Thur Yew,<sup>2</sup> Sergei Krivov,<sup>2</sup> Tom McLeish,<sup>3</sup> and Emanuele Paci<sup>4,a)</sup>

<sup>1</sup>*Institute for Condensed Matter and Complex Systems, School of Physics and Astronomy, University of Edinburgh, Edinburgh, EH9 3JZ, United Kingdom*

<sup>2</sup>*Institute of Molecular and Cell Biology, University of Leeds, Leeds LS2 9JT United Kingdom*

<sup>3</sup>*Departments of Physics and Chemistry, Durham University, Durham DH1 3HP, United Kingdom*

<sup>4</sup>*Institute of Molecular and Cell Biology and School of Physics and Astronomy, University of Leeds, Leeds LS2 9JT, United Kingdom*

(Received 7 April 2010; accepted 2 June 2010; published online 7 July 2010)

Characterizing the conformational properties and dynamics of biopolymers and their relation to biological activity and function is an ongoing challenge. Single molecule techniques have provided a rich experimental window on these properties, yet they have often relied on simple one-dimensional projections of a multidimensional free energy landscape for a practical interpretation of the results. Here, we study three short peptides with different structural propensity ( $\alpha$  helical,  $\beta$  hairpin, and random coil) in the presence (or absence) of a force applied to their ends using Langevin dynamics simulation and an all-atom model with implicit solvation. Each peptide produces fluctuation power spectra with a characteristic dynamic fingerprint consistent with persistent structural motifs of helices, hairpins, and random coils. The spectra for helix formation shows two well-defined relaxation modes, corresponding to local relaxation and cooperative coil to uncoil interconversion. In contrast, both the hairpin and random coil are polymerlike, showing a broad and continuous range of relaxation modes giving characteristic power laws of  $\omega^{-5/4}$  and  $\omega^{-3/2}$ , respectively; the  $-5/4$  power law for hairpins is robust and has not been previously observed. Langevin dynamics simulations of diffusers on a potential of mean force derived from the atomistic simulations fail to reproduce the fingerprints of each peptide motif in the power spectral density, demonstrating explicitly that such information is lacking in such one-dimensional projections. Our results demonstrate the yet unexploited potential of single molecule fluctuation spectroscopy to probe more fine scaled properties of proteins and biological macromolecules and how low dimensional projections may cause the loss of relevant information. © 2010 American Institute of Physics. [doi:10.1063/1.3456552]

Biopolymers have a unique ability to adopt a range of conformations under perturbation allowing them to perform a huge diversity of functions in nature. This arises from the variety of building blocks available in the alphabet of 20 amino acids that compose proteins, resulting in highly complex free-energy landscapes, in sharp contrast to their synthetic analogs. In the past decade single molecule atomic force microscopy (AFM) has been highly successful in characterizing the mechanical properties of many biopolymers and proteins in particular.<sup>1</sup> A typical experiment consists in immobilizing one atom (usually one end) of a protein and retracting a cantilever attached to another atom (usually the other end) at constant speed, and measuring the reaction force  $F$  of the protein as a function of the extension  $x$ ; in the case of stretching protein concatamers measurement of the nonequilibrium unfolding forces allows inference of coarse information about unfolding landscape of proteins. More recently, use of a feedback mechanism, or “force clamp,” has allowed application of constant force  $F$  to single molecules and has been used as an alternative method to calculate global properties of protein unfolding dynamics, such as its relaxation time, as well as studies of protein refolding.<sup>2</sup> How-

ever, recent theoretical and experimental works<sup>3,4</sup> have shown that considerably more information on the energy landscape and the resulting dynamics may be extracted from the spectrum of the fluctuations of the molecule “length,” when held at constant force in single molecule AFM experiments.<sup>5</sup> In principle, by monitoring the dynamics of fluctuations of single proteins with sufficient fidelity of force control, very fine-scaled information on the full unfolding or refolding pathway could be achieved. Currently, the realization of such experiments are complicated and limited by the fact that fluctuations cannot be determined at present in frequency range exceeding hundreds of kilohertz<sup>5</sup> and by the fact that short molecules cannot be studied. On the other hand, molecular dynamics simulations are ideally suited to probing small molecules on short time scales and at atomistic detail. Here we use molecular dynamics simulations to analyze the dynamic fluctuations of short peptides, with differing propensities to form secondary structure such as  $\alpha$  helices and  $\beta$  hairpins or random coils. We investigate the type of information which can be constructed from the power spectral density of molecule extension and compare it to the information available from the commonly used one-dimensional potential of mean force (PMF). We show that heterogeneity in local dynamics of differing peptide se-

<sup>a)</sup>Electronic mail: e.paci@leeds.ac.uk.

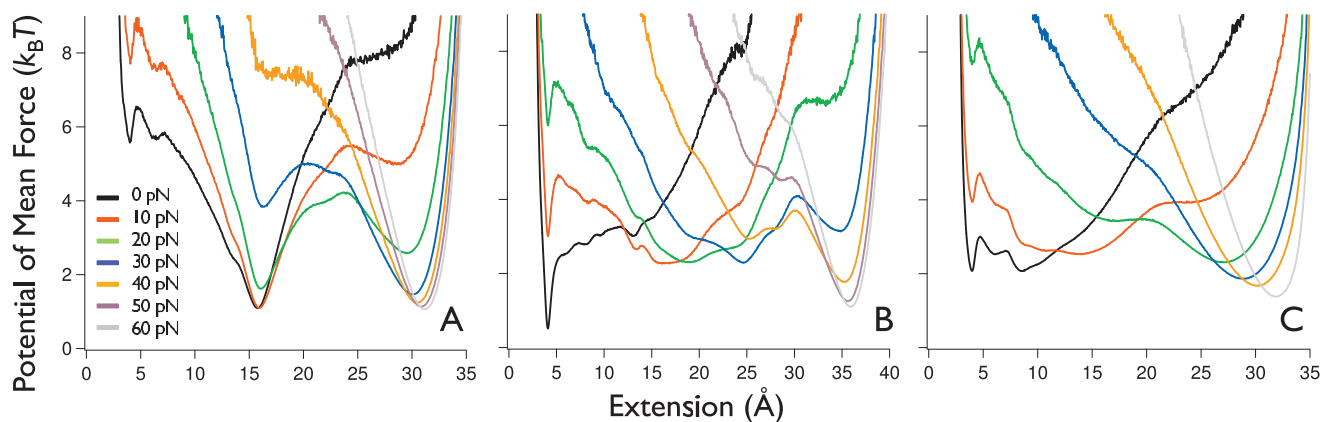


FIG. 1. PMF  $U(x)$  in units of  $k_B T$  at different external forces for (a) peptide A, (b) peptide B, and (c) peptide C, as a function of the end-to-end extension of the peptides.

quences reveal themselves as distinct fingerprints in the power spectrum of fluctuations; in particular, when such states are structured the power spectrum reveals structural motifs. This is in strong contrast to the information contained in the PMF, which we show to be a poor differentiator of the peptide motif structure, highlighting explicitly that reduced dimensional projections, in particular, the one-dimensional PMF of the end-to-end vector, do not correctly reproduce the full many-bodied dynamics of the single molecule.

## I. MODELS AND SIMULATION

Simulations were performed using the CHARMM19 force field with an implicit solvent, which permits equilibrium folding of a large class of structured peptides.<sup>6</sup> A constant force, in the range of 0–60 pN was applied to the ends of the peptides (main-chain nitrogen of the first monomer and carbonyl carbon of last one), oriented as the end-to-end vector. We investigate a 10-alanine (peptide A), a 12-mer with sequence KWYQNGSTKIYT (peptide B), and a 10-glycine (peptide C). With the force field used peptide A has a strong propensity to form helices (77% probability, averaged over all residues, to be in a helical conformation. Peptide B, whose sequence corresponds to the second hairpin of a designed three-stranded  $\beta$  sheet<sup>7</sup> forms a  $\beta$  hairpin (47% probability, averaged over all the residues, to be in an extended conformation, at 300 K and zero force). Peptide C is a random coil, with a residual low propensity to find residues in either helical (6.7%) or extended (22%) conformation. A 2 fs time step was used in all simulations. The length of each trajectory was 2  $\mu$ s. Langevin dynamics with a friction coefficient of 1  $\text{ps}^{-1}$  was used. A limited number of simulations was performed with a higher friction coefficient of 10  $\text{ps}^{-1}$ . Simulations were performed at 300 K temperature.

## II. RESULTS

We simulated suitably short peptides in a range of forces where full convergence of properties such as the distribution of the extension can be achieved. Unlike in single molecule experiments, we can here analyze, in principle, a range of different coordinate-dependent properties, such as the secondary structure. We focus however on the peptides' exten-

sion as this is the quantity which can directly or indirectly monitor, in principle, using atomic force microscopy, optical tweezers, and Foerster resonance energy transfer at a single molecule level.

### A. Static properties

Each simulation produces a time series  $x(t)$  which is the extensional fluctuations of the molecule. The PMF  $U(x)/k_B T = -\ln \rho(x)$  is calculated in each case from a histogram or probability density  $\rho(x)$  of the time series. This is calculated for each force applied to the ends of the peptides and is shown in Fig. 1. For all peptides at large forces  $U(x)$  has a unique minimum corresponding to a highly stretched extended state. For all peptides, as the force is decreased the extended state becomes less stable while more compact states become populated. For peptide A, which we know *a priori* to have a strong helical propensity, a state corresponding to an extension of 15 Å is populated at small forces; while at higher forces the extended state becomes populated. In a relatively broad range of forces both states are populated; equally so at a force around 23 pN. Thus peptide A appears to behave like a two-state system at most forces, and the PMF along the extension appears to describe well its thermodynamic properties.

For peptide B [Fig. 1(b)] there is narrow and deep native state corresponding to an extension of 4 Å populated at small forces. A shallower minimum in the PMF around  $x=4$  Å is actually observed also for peptides A and C and corresponds to conformations where the two ends form a stable contact such as an hairpin or ring. The extended state becomes populated only at forces  $F > 40$  pN. At intermediate forces (7–20 pN) the PMF suggests the existence of a broad intermediate state at extensions between 13 and 20 Å. At intermediate forces we observe shallow minima at intermediate values of the extension which depends on the force.

For peptide C, at all forces except large ones, we see no clear stable state, or at least not a stable state which can be identified by the extension. The extended state, unlike for the two other peptides, becomes thermodynamically stable in the presence of a force as small as 20 pN.

Overall, it is clear for both the force-extension relation and PMF that although there are some differences between

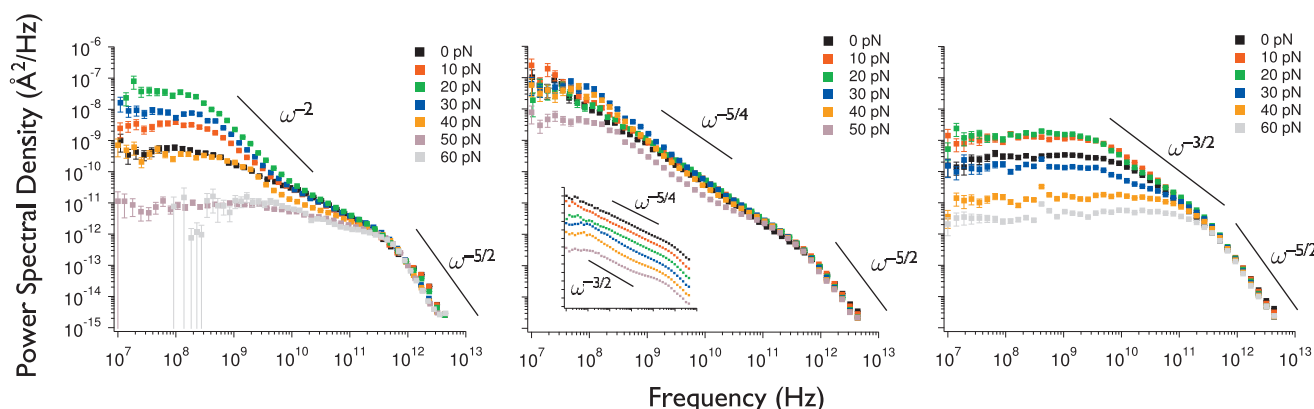


FIG. 2. Power spectral density  $P(\omega)$  of fluctuations from the atomistic simulations on a log-log scale, for forces between 0 and 60 pN, for (a) peptide A, (b) peptide B, and (c) peptide C. The PSD is calculated as indicated in Eq. (2) and then placed in bins on a logarithmic scale so that there is equidistance between points on the log  $\omega$  axis and where each point represents the mean of PSD values in that bin. Error bars are calculated as the standard deviation of PSD values in a given bin and so as there are more points contributing to a given bin at high frequency we find the error decreases.

the different peptides, it is difficult to assign them with confidence with one or another peptide. These essentially static measures hide important differences between the peptides, as we will see below.

## B. Characterizing dynamic properties

We extract from our systems as a coarse-grained variable the extension as a function of the time  $x(t)$ . The time dependent autocorrelation function of this object is defined as

$$C(t) = \langle x(t' + t)x(t') \rangle - \langle x \rangle^2 \quad (1)$$

and can be calculated, where  $\langle \rangle$  represents an ensemble average. The Fourier transform (FT) of this quantity gives the power spectrum density (PSD) of the thermal fluctuations of the end-to-end distance  $P(\omega) = \int C(t)e^{-i\omega t} dt$ . The PSD can be calculated more directly and efficiently by using a fast FT routine on the time series  $x(t)$  and so can also be written as

$$P(\omega) = \lim_{T \rightarrow \infty} \left\{ \frac{\langle |X_T(\omega)|^2 \rangle}{T} \right\}, \quad (2)$$

where  $X_T(\omega) = \int_T x(t)e^{-i\omega t} dt$  is the FT of the time series for a sample of duration  $T$ . In practice,  $T$  is finite and the resolution of the PSD is given by the inverse of this time. The PSD of fluctuations due to thermal noise are intimately connected to the linear response function  $J(\omega)$  of the single molecule through the fluctuation-dissipation theorem,  $P(\omega) = -2k_B T / \omega \text{Im}\{J(\omega)\}$  (Ref. 8) and so provides a direct measure of the dynamics of the molecule.

## C. Comparison of power spectra

The PSDs for each peptide are plotted in Fig. 2 versus frequency on a log-log scale. It is immediately clear that they are markedly different, particularly in the asymptotic power laws exhibited, which are shown for reference. Before we analyze these PSDs further, we ask: does the PSD of fluctuations from the atomistic simulations contain the same information as that contained in the PMF derived from the same fluctuations (as shown in Fig. 1)? We make a simple and

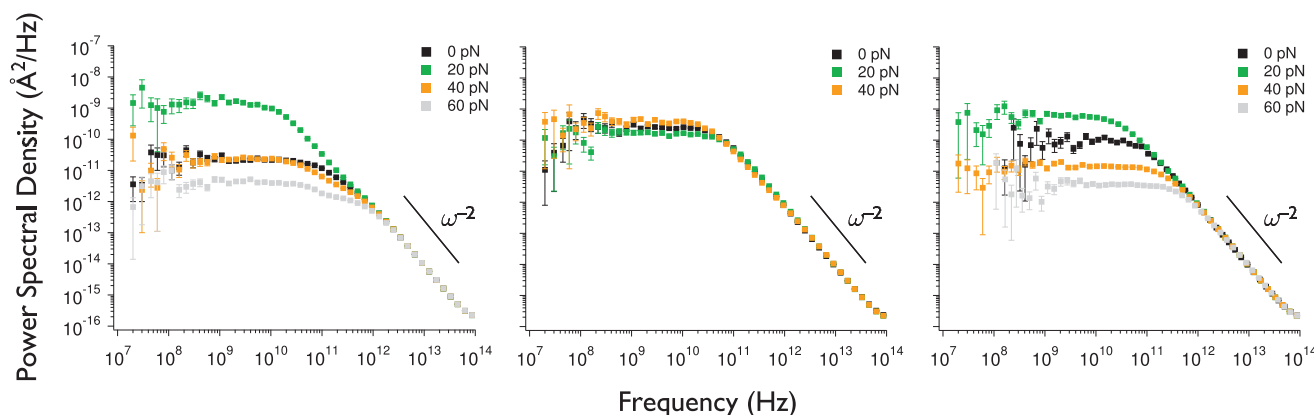


FIG. 3. Power spectral density  $P(\omega)$  obtained by Brownian dynamics on the PMF in Fig. 1, on a log-log scale for forces between 0 and 60 pN, for (a) peptide A, (b) peptide B, and (c) peptide C. The data are binned on a logarithmic scale as in Fig. 2. The scale of friction in these simulations sets the time scale and was chosen to coincide with the friction constant obtained from the fully atomistic simulation for peptide C at  $F=60$  pN, where it is clear the PMF is single well and approximately harmonic; the relaxation time  $\tau$  can be read off from the PSD and the elastic constant  $\kappa$  determined from the PMF [Fig. 1(c)] to give the approximate friction constant  $\zeta = \kappa \tau$  of the atomistic simulations.

qualitative comparison; in Fig. 3 are PSDs calculated from Langevin dynamics simulations of an one-dimensional diffuser on the PMFs shown in Fig. 1, where in each, the panels correspond to the peptides as designated in Figs. 1 and 2. These trajectories are calculated by numerically solving  $(dx/dt) = -(1/\zeta)(d/dx)U(x) + f(t)$ , where  $U(x)$  is the PMF calculated from the atomistic molecular dynamics simulations and shown in Fig. 1,  $x$  is the end-to-end distance of the polymer, and  $f(t)$  represents random thermal noise with zero mean and correlation  $\langle f(t)f(t') \rangle = (2k_B T/\zeta)\delta(t-t')$ . This gives a time series  $x(t)$  from which the PSD is calculated.

Comparing Figs. 2 and 3 it is clear that none of the PSDs from Langevin dynamics on the PMF reproduce the complexity of features in the PSDs that arise from the atomistic level simulations. In particular, as mirrored in the PMFs themselves, the PSDs in Fig. 3 show no strong distinguishing features which would allow identification of high propensity for any particular structural motif. Each of the PSDs show an elastic plateau at low frequency followed by a power law decay of  $\omega^{-2}$ , which is indicative of the dynamics of a simple overdamped spring with a single degree of freedom. It is clear that the simple one-dimensional projection afforded by the PMF cannot encompass information about the dynamics of the molecule along the same one-dimensional projection. Peptide A provides a particular case in point: the PMF is bistable suggesting a separation of time scales between relaxation in each well and relaxation across the barrier, which would give rise to two characteristic relaxation frequencies and two “quasi”-elastic plateaus in the PSD (this can be seen in the PSD from atomistic level simulations). However, this bistability cannot be discerned from the PSD produced from Langevin dynamics on the PMF and can only be recovered by artificially increasing the barrier height. This indicates that the end-to-end distance is not the ideal reaction coordinate as the density of states along this path is underestimated, giving an overestimate of the relaxation frequency for barrier crossing on the PMF.<sup>9,10</sup> So even in the situation where the PMF qualitatively predicts the same response as would be expected from a molecule coiling and uncoiling in a two-state manner, such predictions are not quantitative.

#### D. Power spectra from atomic level simulations

In general, molecules such as peptides are objects with a number of degrees of freedom, such as polymers or rods, whose response or fluctuations can be decomposed into normal modes, each of which relaxes in a single-mode manner at some characteristic frequency  $\tau_q$  and with some elastic constant  $\kappa_q$ ,

$$J_q(\omega) = \frac{1}{\kappa_q(1 + i\omega\tau_q)} \quad (3)$$

where the real part of  $J_q$  is the elastic or in-phase part of the response and the imaginary part is the dissipative or out-of-phase response. The exact dispersion relations  $\kappa_q$  and  $\tau_q$  of a given molecule will depend on the static and dynamic structures of the object, which manifest themselves as different characteristic power laws in the total response of the molecule, which is a sum over modes. For example, a flexible

polymer is often modeled using the Rouse model,<sup>11</sup> whose dispersion relations with mode number  $q$  are  $\kappa_q \sim \kappa q^2$  and  $\tau_q = \tau/q^2$ —summing over all modes gives a total response function that decays at high frequency as  $\omega^{-1/2}$  or in the PSD as  $\omega^{-3/2}$ . Here we probe the PSD for each type of peptide and at a range of forces as shown in Fig. 2. As noted above different power laws clearly emerge, which we analyze below.

First, the PSDs of all peptides show two common features: (1) a plateau at low frequency indicating the dominance of elastic processes and (2) a common asymptotic power law of with an exponent less than  $-2$  at very high frequency ( $\nu > 10^{12}$  Hz, where  $\nu = 2\pi\omega$ —fits in this frequency regime to  $\log[P(\omega)] = \alpha - \gamma \log(\omega)$ , give an exponent  $\gamma$  between  $5/2$  and  $3$ , across all peptides). This high frequency regime is interesting, since we would expect a law of  $-2$ , corresponding to the overdamped dynamics of internal frictional processes that dominate short wavelength modes.<sup>3</sup> Given this regime only spans at most one order of magnitude in frequency and that there will be aliasing at the Nyquist frequency, discussing the quantitative values of the exponents is not very meaningful; however, as a possible explanation for a deviation from  $-2$  behavior, we note that an exponent in the PSD of  $-5/2$  corresponds to an extra power-law contribution of  $\omega^{1/2}$ , which recalls high frequency corrections to far-field Stokes friction.<sup>12</sup> However, here we suggest the effective solvent may arise from the multiple higher-frequency internal modes of the peptides, which will create an effective viscous contribution of frequency-dependent magnitude. But whatever its origin, this phenomenon cannot be produced from PSDs derived from Langevin dynamics on the PMFs (Fig. 3), which uniformly exhibit an asymptotic power law of  $-2$  at high frequency.

The PSDs for peptide A [Fig. 2(a)] in general exhibit the superposition of a slow and fast mode with two distinct relaxation frequencies and a strong dependence on the applied force. An exponent of  $-2$  in the PSD would indicate single-mode behavior with a single well defined relaxation time; for the slow mode this only approximately obeyed due to the close proximity of the fast mode, while for the fast mode we find a modified exponent less than  $-2$ , as discussed above. The existence of two well defined relaxation frequencies is qualitatively consistent with the picture obtained from the PMF of an equilibrium between helical and extended states; we expect the fast time to be related to relaxation in the local minima corresponding to the helical and extended states, while the slow time is related to relaxation of motions that go between helical and extended states. As force increases from 0 pN the slow interwell mode contribution to the PSD becomes increasingly smaller, as the underlying PMF becomes less bistable and more single wellled, up to approximately (50 pN) when the PSD is essentially single mode. However, despite a qualitative agreement of features in the PSD with features in the PMF, as we have seen the information in the PMF is not sufficient to quantitatively reproduce the PSD in Fig. 2(a).

For peptide B [Fig. 2(b)] at forces less than 30 pN, we measure a power law dependence of  $-5/4$  of its PSD over more than four decades in frequency ( $10^7 \text{ s}^{-1} < \nu$



$< 10^{11} \text{ s}^{-1}$ , where for  $F=\{0, 10, 20\}$  pN the measured exponents are  $\gamma=\{1.26 \pm 0.01, 1.26 \pm 0.01, 1.25 \pm 0.01\}$ , respectively, where errors are calculated from the linear regression). The origin of the  $-5/4$  exponent ( $-1/4$  in the imaginary part of the response function) is not known, but it likely arises from the dynamics of the hairpin as it explores a wide range of hairpinlike conformations with fluid, or solventlike, degrees of freedom (i.e., with very small barriers of interconversion). In principle, such an exponent should be calculable from a microscopic model of beta hairpin dynamics (e.g., Ref. 13) or from more coarse-grained modeling.<sup>14</sup> At this point we observe that a polymer with fractal dimension  $d_f$  and local dissipation exhibits a power-law power spectrum  $P(\omega) \sim \omega^{-\gamma}$  with  $\gamma=1+d_f/(d_f+2)$  (B.K., Z.T.Y., T.C.B.M., and E.P., manuscript in preparation). A model with  $d_f$  between 1 and 2 describes a chain with a distribution of side loops controlled by strongly local friction. This can arise for example in the case of breaking and reforming hydrogen bonds. Such a model is consistent with power-spectrum exponent  $\gamma$  smaller than  $3/2$  ( $d_f=2$ ), the power law we find below for a random coil (peptide C), and that expected for the Rouse model;<sup>4,11</sup> in particular, a fractal dimension  $d_f=1$  gives a power law exponent  $\gamma=4/3$ , which is close to the observed exponent. We note that for simulations that probe significantly lower frequencies (longer times) we may expect to see a folding plateau emerge at lower frequency, similar to that seen for helices for  $\nu < 10^8$  Hz. This would be consistent with experimental folding times of hairpins being 1–2 orders of magnitude slower than helices.<sup>15</sup> At larger forces ( $F \geq 30$  pN) we find an elastic plateau at low frequencies followed by a power law which is instead approximately  $-3/2$ , the exponent for a random coil. In particular, in the frequency range of approximately  $10^8 \text{ s}^{-1} < \nu < 10^{10} \text{ s}^{-1}$ , we measured exponents of  $\gamma=\{1.48 \pm 0.02, 1.49 \pm 0.03, 1.29 \pm 0.03\}$ , for  $F=\{30, 40, 50\}$  pN, respectively, where the measurement at 50 pN is expected to be less reliable as the range of frequency over which the power law extends is reduced, as seen in Fig. 2. Overall, we see here that changes in the PSD provides a sensitive signal that there is a transition at approximately 30 pN, where the hairpin denatures subsequently exhibiting random coil dynamics.

At low forces ( $< 30$  pN), the PSD of the unstructured peptide C exhibits an elastic plateau at low frequency followed by a power law of approximately  $-3/2$ ; for a frequency range of  $10^{10} \text{ s}^{-1} < \nu < 3 \times 10^{11} \text{ s}^{-1}$ , we find  $\gamma=\{1.50 \pm 0.03, 1.50 \pm 0.02, 1.30 \pm 0.03\}$  for  $F=\{0, 10, 20\}$  pN, respectively. The measurement for  $F=20$  pN, we again expect that it is less reliable as the power law regime becomes less well defined as the low frequency plateau weakens to give single-mode behavior at high force. An exponent of  $-3/2$  would arise from the many degrees of freedom of a simple freely jointed polymer in a solvent; as mentioned above the PSD for a such an object is predicted by the Rouse model to follow a  $-3/2$  power law. However, in general it is expected that for short polymers, when the molecular weight of the polymer,  $N \ll \sqrt{\zeta_{i0}/\zeta_{s0}}$ , internal friction dominates<sup>3,16</sup> giving single-mode overdamped relaxation, where  $\zeta_{i0}$  and  $\zeta_{s0}$  are the monomeric friction constants for internal and solvent dissipation, respectively. For this power law to arise for short

peptides it is necessary for the friction constant per monomer due to solvent motion to be at least within a couple of orders of magnitude of the constant for internal friction<sup>4</sup> [for typical biopolymers at high stretch,  $\zeta_{i0}/\zeta_{s0} \sim 10^6$  (Refs. 3 and 17)]. As the chain is at moderate stretch for  $F < 30$  pN ( $F\ell_p \sim k_B T$ , where  $\ell_p \sim 3 \text{ \AA}$  is the typical persistence length of a polypeptide chain), we suggest that in order for the same mechanism to be at play in this unstructured peptide, here, the dynamics arises from friction with the effective solvent formed from non-nearest neighbor monomer-monomer interactions of the single peptide. This monomer solvent would give an effective friction constant of the same order of magnitude as for internal friction, since they are due to the same underlying interactions and so we would expect to see a  $-3/2$  power law at low frequencies indicative of the relaxation of polymeric degrees of freedom. For forces  $F > 30$  pN, we see that the PSD across all frequencies tends to the behavior of a single-mode overdamped spring indicating that internal friction dominates the dynamics of all modes. This is consistent with a decreasing monomer-monomer solvent contribution as the chain is stretched and an internal friction constant increasing monotonically with force, which is a general prediction for polymers at high stretch<sup>3,17</sup> and arises as consequence of a decreased dynamical flexibility of the chain under increasing tension.

It is interesting to contrast the behavior of peptide A compared to peptides B and C, since the latter present dynamics consistent with the null hypothesis that a short peptide is a polymer with many degrees of freedom which have very small barriers to interconversion to different conformations. Peptide A, on the other hand, presumably because of the special relationship of interactions between its amino acid backbone, has lost its polymer properties and populates, with a high degree of cooperativity, a relatively narrow ensemble of states that constitute a helix. The highly cooperative transition of the alpha helix is of course well known.<sup>18,19</sup> However, despite this large cooperativity and consequent dimensional reduction, as we have seen the PMF of the end-to-end distance cannot correctly capture the dynamics of the molecule.

### III. DISCUSSION

Polypeptides, even short ones, have a free-energy landscape which while simpler than for a larger protein, contains the same type of complexity. Such complexity is due to the large number of metastable states and rich dynamics of transitions between them, which are in turn due to the complex interplay between a large number of possible favorable interactions between atoms, and entropy loss upon formation of such structures. Experimental characterization of free-energy surface is challenging because of the limited number of probes that can be monitored on a broad range of time scales. Even atomistic simulations, where any single molecule observable can be monitored with arbitrary time resolution pose serious challenges when one attempts to represent the free-energy surface and insightfully describe the dynamics of the system.

Many single molecule techniques, such as atomic force

microscopy, probe only the extension. It has been hinted previously that extension is not in general a good reaction coordinate for unfolding,<sup>20</sup> and this is particularly the case when no, or only a small, force is applied. Indeed, the evolution of single molecule techniques which provide a time series has sparked the development of empirical methods<sup>21,22</sup> to extract information on the underlying free-energy landscape even if the quantity monitored does not have the properties of a good reaction coordinate. In simulation one can detect the existence of states from an analysis of the trajectory in the conformation space, but even in that case this is not straightforward.<sup>23,24</sup> The peptides studied here provide an excellent example of this problem, despite their simplicity. While for peptide A, the PMF of the extension,  $U(x)$ , provides strong hints on the existence and nature of well-defined basins in the free-energy landscape (when determined at different forces), for peptides B and C it has little information on the free-energy landscape (at least at low or intermediate forces) and the many-body effects that give rise to the characteristic power laws observed in the PSDs. To show this explicitly, we conducted Brownian dynamics simulations of a diffuser on the PMFs derived from the fully atomistic simulations. The resultant PSDs of the time series cannot reproduce the dynamics of the fully atomistic simulations, even in the case of peptide A, and instead produce the dynamics of a simple overdamped spring with first order kinetics ( $\omega^{-2}$ ). To be completely rigorous, in projecting onto the one-dimensional PMF, a coordinate dependence of diffusion should be extracted.<sup>24,25</sup> The coordinate dependent diffusion coefficient, in particular, can change the position of the transition state,<sup>26</sup> or even change the number of basin.<sup>24</sup> Employing the approach described in Ref. 24 the coordinate dependent diffusion coefficient can be found as  $D(x) = (\pi/\Delta t) \times [Z_C(x)/Z_H(x)]^2$ , where  $\Delta t$  is the sampling interval and  $Z_C(x)$  and  $Z_H(x)$  are the partition function of the cut based and conventional (histogram) free energy profiles.  $Z_C$  at point  $x$  is defined as the number of transitions through that point, i.e.,  $Z_C(x) = 1/2 \sum_t \Theta\{[x(t) - x][x - x(t + \Delta t)]\}$ , where  $\Theta\{x\}$  is the Heaviside step function.  $Z_H(x)$  is determined by computing a histogram as  $Z_H(x) = N_x/\Delta X$ , where  $N_x$  is the number of time-series points in bin  $x$  and  $\Delta X$  is the size of the bin. The analysis shows that the diffusion coefficient varies only marginally; for example, for peptide A at zero force it varies between 0.1 and 0.15. As a consequence, the PSD computed from the diffusive dynamics with the coordinate dependent diffusion coefficient is almost indistinguishable from that with coordinate independent diffusion coefficient. This brings to fore the essential point that the phenomenon we observe specifically requires the interplay between the many degrees of freedom of the polymer, as embodied in Eq. (3) and how the dynamics varies on different length scales, embodied in the specific elastic and friction dispersion relations  $\kappa_q$  and  $\zeta_q$ . Similarly, there exist complementary methods that attempt to analyze the complexity of the multidimensional energy landscape, for example, by looking at fluctuations in the total potential energy in time,<sup>27,28</sup> however, these studies show that the emergent fractal behavior is

insensitive to global dynamics and only represent intermode coupling from anharmonicity of the local potentials.

In conclusion, when the power spectra of the fully atomistic simulations is analyzed, we discover rich phenomena with information which complements and exceeds that contained in the PMF. In particular, we have seen that the many-bodied dynamics of peptides leads to the emergence of distinct fingerprints for the power spectra of helices, hairpins, and random coils and the detection of transitions between them. Combining theory, simulation, and experiments that analyze the dynamical fluctuations of single biomolecules holds promise of experimental observation of such motifs and their transitions, for example, during the unfolding or refolding of proteins and opens a new window on the properties of disordered or partially structured proteins.

## ACKNOWLEDGMENTS

We acknowledge Igor Neelov for discussions in the early stages of the project. Z.T.Y. and E.P. acknowledge Wellcome Trust for financial support.

- <sup>1</sup>M. Rief and H. Grubmüller, *ChemPhysChem* **3**, 255 (2002).
- <sup>2</sup>J. M. Fernandez and H. Li, *Science* **303**, 1674 (2004).
- <sup>3</sup>B. S. Khatri, M. Kawakami, K. Byrne, D. A. Smith, and T. C. McLeish, *Biophys. J.* **92**, 1825 (2007).
- <sup>4</sup>B. S. Khatri and T. C. B. McLeish, *Macromolecules* **40**, 6770 (2007).
- <sup>5</sup>M. Kawakami, K. Byrne, B. Khatri, T. C. McLeish, S. E. Radford, and D. A. Smith, *Langmuir* **20**, 9299 (2004).
- <sup>6</sup>P. Ferrara, J. Apostolakis, and A. Caffisch, *Proteins* **46**, 24 (2002).
- <sup>7</sup>E. de Alba, J. Santoro, M. Rico, and M. A. Jimenez, *Protein Sci.* **8**, 854 (1999).
- <sup>8</sup>P. Chaiken and T. Lubensky, *Principles of Condensed Matter Physics* (Cambridge University Press, Cambridge, 1995).
- <sup>9</sup>D. Chandler, *J. Chem. Phys.* **68**, 2959 (1978).
- <sup>10</sup>D. Frenkel and B. Smit, *Understanding Molecular Simulation*, 2nd ed. (Academic, New York, 2002).
- <sup>11</sup>P. Rouse, *J. Chem. Phys.* **21**, 1272 (1953).
- <sup>12</sup>L. D. Landau and E. Lifshitz, *Fluid Mechanics*, 2nd ed. (Pergamon, New York, 1987).
- <sup>13</sup>V. Muñoz, E. R. Henry, J. Hofrichter, and W. A. Eaton, *Proc. Natl. Acad. Sci. U.S.A.* **95**, 5872 (1998).
- <sup>14</sup>T. X. Hoang, A. Trovato, F. Seno, J. R. Banavar, and A. Maritan, *Proc. Natl. Acad. Sci. U.S.A.* **101**, 7960 (2004).
- <sup>15</sup>V. Muñoz, P. A. Thompson, J. Hofrichter, and W. A. Eaton, *Nature (London)* **390**, 196 (1997).
- <sup>16</sup>P. G. de Gennes, *Scaling Concepts in Polymer Physics* (Cornell University Press, Ithaca, 1985).
- <sup>17</sup>B. S. Khatri, K. Byrne, M. Kawakami, D. J. Brockwell, D. A. Smith, S. E. Radford, and T. C. B. McLeish, *Faraday Discuss.* **139**, 35 (2008).
- <sup>18</sup>B. H. Zimm and J. K. Bragg, *J. Chem. Phys.* **31**, 526 (1959).
- <sup>19</sup>B. Chakrabarti and A. J. Levine, *Phys. Rev. E* **74**, 031903 (2006).
- <sup>20</sup>Z. T. Yew, S. Krivov, and E. Paci, *J. Phys. Chem. B* **112**, 16902 (2008).
- <sup>21</sup>A. Baba and T. Komatsuzaki, *Proc. Natl. Acad. Sci. U.S.A.* **104**, 19297 (2007).
- <sup>22</sup>H. Li, H. C. Wang, Y. Cao, D. Sharma, and M. Wang, *J. Mol. Biol.* **379**, 871 (2008).
- <sup>23</sup>S. V. Krivov and M. Karplus, *Proc. Natl. Acad. Sci. U.S.A.* **101**, 14766 (2004).
- <sup>24</sup>S. V. Krivov, S. Muff, A. Caffisch, and M. Karplus, *J. Phys. Chem. B* **112**, 8701 (2008).
- <sup>25</sup>R. B. Best and G. Hummer, *Proc. Natl. Acad. Sci. U.S.A.* **107**, 1088 (2010).
- <sup>26</sup>J. Chahine, R. J. Oliveira, V. B. Leite, and J. Wang, *Proc. Natl. Acad. Sci. U.S.A.* **104**, 14646 (2007).
- <sup>27</sup>D. A. Lidar, D. Thirumalai, R. Elber, and R. B. Gerber, *Phys. Rev. E* **59**, 2231 (1999).
- <sup>28</sup>M. S. Li, M. Cieplak, and N. Sushko, *Phys. Rev. E* **62**, 4025 (2000).